





Improving Performance of Silicon Thermo-Optic Switch by Combing Spiral Phase Shifter and Optimized Pulse Driving

Dongdong Lin, Wei Cheng, Shangqing Shi, Pengcheng Liu , Mengjia Lu, Tong Lin, Guohua Hu ,
Binfeng Yun , and Yiping Cui 

Abstract—For the silicon photonics integrated circuits, the optical switch plays a vital role in many applications. Large scale integration requires low switching power and fast switching speed. However the switching time and switching power of silicon thermo-optic switch are typically limited to tens of micro-seconds and tens of milli-watts, respectively. In this paper, we designed and fabricated a silicon thermo-optic switch with spiral optical phase shifters, which can reduce the switching power from 21.5 mW to 8.73 mW compared to the optical switch with straight phase shifters. Furthermore, we optimized the pulse driving, we proposed the calculation formula of the pulse voltage, and the overall quantitative scheme of the pulse voltage and pulse width. By adopting the optimized pulse driving, the switching time is reduced from 27 μs to 4 μs . The proposed silicon thermo-optic switch unit with optimized pulse driving is very promising for the applications where large scale integration of optical switches is needed.

Index Terms—Silicon photonics, optical switch, thermo-optic, switching time, switching power.

I. INTRODUCTION

SILICON photonics has the advantages of low insertion loss, high integration capability and compatibility with the complementary-metal-oxide-semiconductor (CMOS) fabrication processes, make it suitable for large scale optical integration [1]–[4]. Silicon optical switches play a vital role in many applications such as optical delay line [5]–[7], optical switch matrix [8] and quantum optics [9], etc. Typically, silicon optical switch can be realized by Mach-Zehnder interferometer (MZI) with tunable optical phase shifter, which can be achieved by using the well-known carrier dispersion [10], [11] and thermo-optic (TO) effects [12]–[21]. Silicon optical switch based on the carrier dispersion can achieve very fast switching speed down to sub-nanoseconds. However, since optical absorption

coefficient of silicon will be changed simultaneously during phase shifting, which will deteriorate the extinction ratio and insertion loss of MZI optical switch. Furthermore, active silicon photonic fabrication process is needed, which is costly. By contrast, silicon TO switch can overcome these shortcomings to achieve high extinction ratio and low loss. But the switching time and switching power of silicon TO switch are typically limited to tens of micro-seconds and tens of milli-watts, respectively. The relative low switching speed and high switching power limit its applications, especially in large scale silicon photonic integration scenarios. To reduce the switching power, one approach is to create air-gap trenches or adopt silicon undercut process to reduce unwanted heat dissipation [12], [13]. However, this will introduce additional processes and dramatically increase switching time. Another effective approach is optimizing the optical phase shifter by using folded optical waveguides to increase the heat utilization. In [14], a TO switch with highly dense routing of 9 waveguides under a 10 μm wide heater was demonstrated, and a low switching power of 3.8 mW was achieved with air-gap trench, however the switching time was above 45 μs due to the poor heat conduction of air. In [15], by geometrical design optimization, an optical phase shifter consumes 2.56 mW for π phase shift was proposed, but the switching time was above 34.8 μs . In [16], a TO phase shifter based on a densely distributed silicon spiral waveguide with switching power of 3 mW was demonstrated and the switching time of about 11 μs was obtained, but still above 10 μs . On the other hand, in [17], a differential control method was proposed to accelerate the TO switch's switching speed and sub-microsecond switching time was achieved, but the switching power consumption was large because both heaters were in the same higher temperature state. In [18], a pulse-width modulation with “Turbo Pulse” was used to reduce the TO switch's switching time to 5.8 μs , but the amplitude and width of the “Turbo Pulse” need to be further optimized quantitatively, and the switch's switching power was not improved with conventional straight optical phase shifter. As can be seen, few silicon TO switch can get sub-10 mW switching power and sub-10 μs switching time simultaneously.

In this paper, we designed and fabricated a silicon TO switch with spiral optical phase shifters, by adopting the spiral phase shifters instead of straight phase shifters, the switching power

Manuscript received March 15, 2022; revised April 6, 2022; accepted April 6, 2022. Date of publication April 11, 2022; date of current version April 26, 2022. This work was supported in part by the National Key R&D Program of China under Grant 2018YFB2201800, in part by the National Natural Science Foundation of China under Grant 62171118, and in part by the National Natural Science Foundation of China under Grant 62105061. (Corresponding author: Binfeng Yun.)

The authors are with the Advanced Photonics Center, Southeast University, Nanjing 210096, China (e-mail: 230189508@seu.edu.cn; 230208634@seu.edu.cn; 220191328@seu.edu.cn; 230189112@seu.edu.cn; mjlu@seu.edu.cn; linton@seu.edu.cn; photonics@seu.edu.cn; ybf@seu.edu.cn; cyp@seu.edu.cn).
Digital Object Identifier 10.1109/JPHOT.2022.3166167

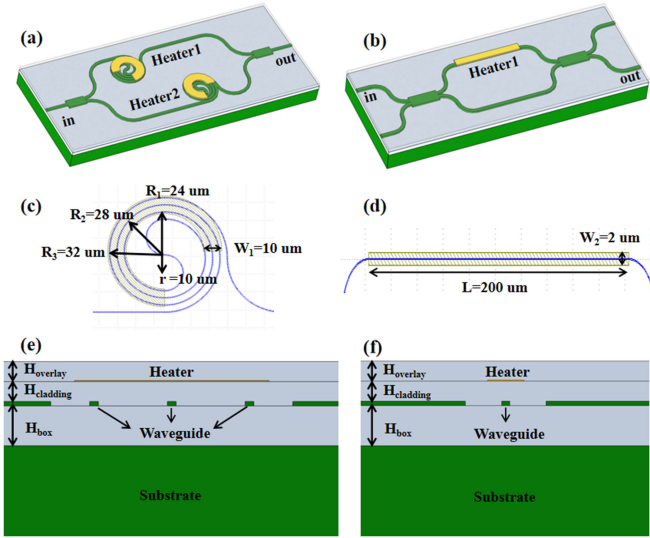


Fig. 1. (a) The schematic diagram of MZI TO switch with spiral optical phase shifters. (b) The schematic diagram of MZI TO switch with straight optical phase shifter. (c) The schematic diagram of designed spiral optical phase shifter. (d) The schematic diagram of designed straight optical phase shifter. (e) The cross section of spiral optical phase shifter. (f) The cross section of straight optical phase shifter.

can be reduced from 21.5 mW to 8.73 mW. We also optimized the pulse driving, we proposed the calculation formula of the pulse voltage in the cooling process, and then the overall quantitative scheme of the pulse voltages and pulse widths in both cooling and heating processes. By adopting the optimized pulse driving, the switching time is reduced from 27 μ s to 4 μ s. By combing spiral phase shifter and optimized pulse driving, our TO switch can get sub-10 mW switching power and sub-10 μ s switching time simultaneously.

II. THEORETICAL MODEL

A. Reduce Switching Power By Spiral Optical Phase Shifter

The schematic diagram of the designed MZI TO switch with spiral optical phase shifters is shown in Fig. 1(a). The optical phase shifters are both formed by spiral waveguides which are covered by TiN heating electrodes to tune the mode effective refractive indices, then the optical phases by TO effect. The detail structure of the designed spiral optical phase shifter is shown in Fig. 1(c). According to the design manual and our simulation, the gap between the waveguides should be larger than 3 μ m to avoid optical coupling, the radius of waveguide bend should be larger than 8 μ m to ensure that the bending loss is low enough to be neglected. On the other hand, to improve the integration density for the scenarios where large amount of TO switches is needed in a single chip, for example, the optical beamforming network by cascaded TO switch delay line or large scale optical switch matrix, the size of the TO switch should be as compact as possible. Based on the above considerations and the possible manufacturing errors, we set the gap between the spiral waveguides as 4 μ m to ensure the optical coupling will not occur, set the inner radius of the spiral waveguide as $r = 10 \mu$ m

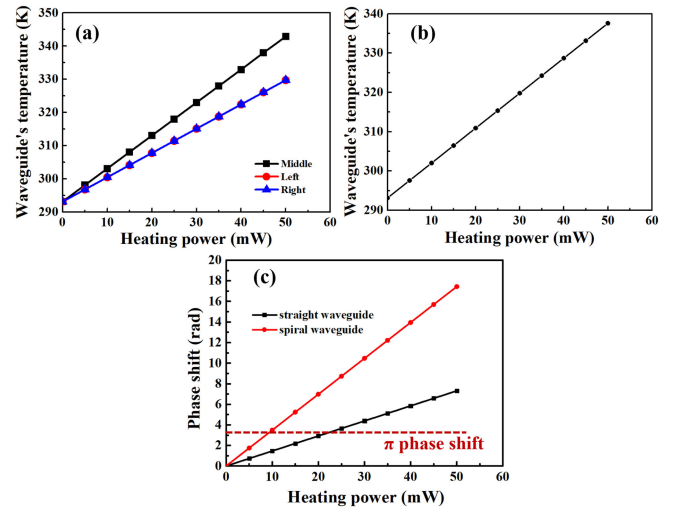


Fig. 2. (a) The relation between the spiral waveguide's temperature and heating power. (b) The relation between straight waveguide's temperature and heating power. (c) The comparison of the phase shifts between the spiral and straight waveguide with varying heating power.

to ensure that the bending loss is low enough to be neglected, and also make the TO switch compact as well. The heater width is set as $w_1 = 10 \mu$ m to cover most of the spiral waveguides. The cross section of spiral optical phase shifter is shown in Fig. 1(e), where the thicknesses of the buried oxide (BOX), SiO₂ cladding and SiO₂ overlay are $H_{\text{box}} = 2 \mu$ m, $H_{\text{cladding}} = 1 \mu$ m and $H_{\text{overlay}} = 1 \mu$ m, respectively. The cross section of the silicon waveguide is set as 220 nm \times 450 nm to ensure single mode operation. For the 1 \times 1 MZI TO switch shown in Fig. 1(a), the output will reach maximum (“on” state) when the phase difference between the two arms is 0 or 2π due to constructive interference, while output reaches minimum (“off” state) when phase difference between the two arms is π . As comparing, a normal 2 \times 2 MZI TO switch with straight optical phase shifter is designed in the same chip, and its schematic diagram is shown in Fig. 1(b). The detail structure of the designed straight optical phase shifter is shown in Fig. 1(d), where the heater width is set as $W_2 = 2 \mu$ m. The cross section of straight optical phase shifter is shown in Fig. 1(f). Just as the 1 \times 1 MZI TO switch with spiral optical phase shifter, if light is input from the “in” port, the optical output from the “out” port reaches the maximum and minimum when the phase differences between the two arms are 0 and π , respectively.

In order to compare the switching power between the silicon MZI TO switches with spiral and straight optical phase shifters, two dimensional thermo-optic simulations of the optical phase shifters were carried out as shown in Fig. 1(e) and (f) to obtain the waveguides' temperatures with varying driving powers. The initial temperature is set as $T_0 = 293.15$ K. By scanning the driving power on heater1 of the spiral optical phase shifter from 0 mW to 50 mW with step of 5 mW, the waveguides' temperatures after heating are shown in Fig. 2(a), the red curve which denotes the temperature of the left waveguides overlaps with the blue curve which denotes the temperature of the right

waveguides, in other words, the temperatures of both the left and right waveguides shown in Fig. 1(e) are the same, and lower than the temperature of the middle waveguide. The straight waveguide's temperature after heating was also simulated and shown in Fig. 2(b). According to the TO effect, the refractive index of silicon after heating can be expressed as

$$n_{si} = n_{si} + \frac{dn_{si}}{dT}(T - T_0) \quad (1)$$

Where $n_{si} = 3.476$ is the refractive index of silicon at 293.15 K, $dn_{si}/dT = 1.86 \times 10^{-4} 1/K$ is the TO coefficient of silicon. By using the silicon refractive indices at different temperatures obtained by Eq. (1), the TE mode effective refractive indices (n_{eff}) of the silicon waveguide at different temperatures were obtained. Then the waveguide's phase shift caused by electrode heating were obtained with the following equation:

$$\Delta\phi = \frac{2\pi}{\lambda}(n_{eff} - n_{eff0})L \quad (2)$$

Where n_{eff0} is the TE mode effective refractive index at 293.15 K, n_{eff} is the TE mode effective refractive index after heating, L is the length of the heated waveguide and λ is set as 1550 nm. The lengths of the three silicon spiral waveguides covered by the heating electrode are 150.72 μm , 175.84 μm and 200.96 μm , respectively. According to (1) and (2), the relations between the phase shifts and driving powers of the two kinds of optical phase shifters were obtained and shown in Fig. 2(c). It can be seen that driving powers of about 9.0 mW and 22 mW are needed to achieve π phase shift for optical switching with the spiral and straight optical phase shifters, respectively. The simulation results show that the designed spiral optical phase shifter can reduce the switching power by 59%.

B. Accelerate Switching Speed By Optimized Pulse Driving

In order to accelerate the switching speed, pulse driving could be applied [18], but the pulse voltage and pulse width need to be further optimized quantitatively. The optical switching process can be divided into heating (“off” to “on”) and cooling (“on” to “off”) processes. Here we proposed the calculation formula of the pulse voltage V_P in the cooling process firstly, based on the value of V_P , we can get the overall quantitative scheme of pulse voltage and pulse width in both cooling and heating processes to optimize the pulse driving. An appropriate pulse was applied to the heater2 to accelerate the cooling process firstly and the working principle is illustrated in Fig. 3. As shown in Fig. 3(a), when only the voltage applied to the heater1 changes from “ V_{on} ” to “ V_{off} ” at t_1 , the switch will change from the “on” state to the “off” state gradually due to the phase difference between the waveguide1 and the waveguide2 changes from 2π to π by just cooling of waveguide1. In other words, this means $\Phi_1 - \Phi_4 = 2\pi$, $\Phi_3 - \Phi_4 = \pi$ should be satisfied in Fig. 3(b) and (d). So the corresponding switching time from the “on” state to the “off” state will be $(t_3 - t_1)$ if no pulse voltage is applied to the heater2. However, when the voltage “ V_{on} ” on the heater1 drops, if we apply a pulse with appropriate voltage V_P and pulse width of $(t_2 - t_1)$ to the heater2 as shown in Fig. 3(c), an additional phase

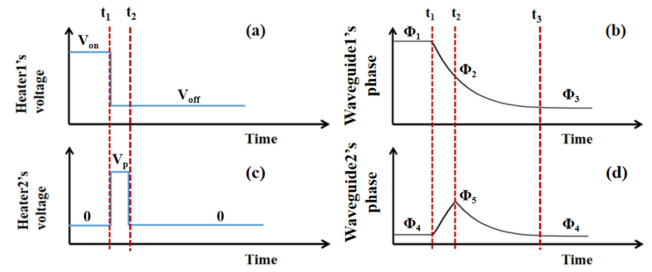


Fig. 3. (a) The schematic diagram of the driving voltage applied on the heater1 in the cooling process. (b) The schematic diagram of waveguide1's phase in the cooling process. (c) The schematic diagram of the pulse applied on the heater2 in the cooling process. (d) The schematic diagram of waveguide2's phase with pulse driving in the cooling process.

change of waveguide2 as shown in Fig. 3(d) will be introduced to reduce the phase difference between the waveguide1 and waveguide2. Through optimizing V_P and $(t_2 - t_1)$, the TO switch's cooling process can be accelerated from $(t_3 - t_1)$ to $(t_2 - t_1)$. To keep the switch's “off” state after t_2 , the phase difference between waveguide1 and waveguide2 should be kept as π from t_2 , which requires $\Phi_2 - \Phi_5 = \pi$, and the phase changing of waveguide1 and waveguide2 should be same during $t_2 \sim t_3$. To meet this requirement, the heating power applied to waveguide1 and waveguide2 should be same, so we can determine the driving pulse voltage V_P as the following equation:

$$\frac{V_P^2}{R_2} = \frac{V_{on}^2 - V_{off}^2}{R_1} \quad (3)$$

Where R_1 and R_2 represent the resistances of the heater1 and the heater2, respectively. Once the driving pulse voltage V_P on the heater2 is obtained by (3), the pulse width $(t_2 - t_1)$ could be determined as long as the phase difference between waveguide1 and waveguide2 is π at t_2 when the pulse ends. In our following experiments, by setting the pulse width $(t_2 - t_1)$ properly, the switch's output will be minimum at t_2 , in other words, the switch will reach the “off” state as soon as the pulse ends. This is the criterion to determine the pulse width $(t_2 - t_1)$.

On the other hand, we also introduce a pulse to accelerate the heating process and the working principle is illustrated in Fig. 4. When the heater1's voltage rises from “ V_{off} ” to “ V_{on} ”, the waveguide1's phase changes from Φ_3 to Φ_1 as shown in Fig. 4(b), the phase difference between waveguide1 and waveguide2 changes from π to 2π . If we applied a pulse with voltage V_{ph} which is higher than “ V_{on} ” as shown in Fig. 4(c), the waveguide1's phase will change faster as shown in Fig. 4(d) and the switch's heating process can be accelerated. The larger V_{ph} is, the faster the heating time. However, over heating will occur if too large V_{ph} is applied and has the risk of fusing heaters. So the pulse voltage and pulse width need to be optimized. In our following experiments, our criterion for determining pulse amplitude V_{ph} and pulse width Δt is based on the cooling time, since the accelerated cooling time $(t_2 - t_1)$ could be determined, if the V_{ph} with pulse width Δt can accelerate the heating time less than or equal to the cooling time, we can say that the V_{ph} with pulse width Δt is enough to reduce the overall switching time to $(t_2 - t_1)$.

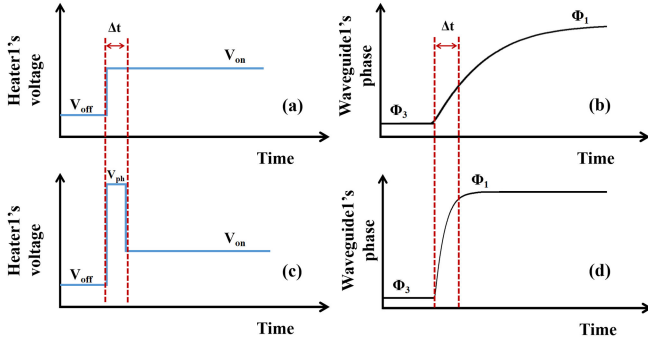


Fig. 4. (a) The schematic diagram of the driving voltage applied on the heater1 without pulse driving in the heating process. (b) The schematic diagram of waveguide1's phase without pulse driving in the heating process. (c) The schematic diagram of the pulse applied on the heater1 in the heating process. (d) The schematic diagram of waveguide1's phase with pulse driving in the heating process.

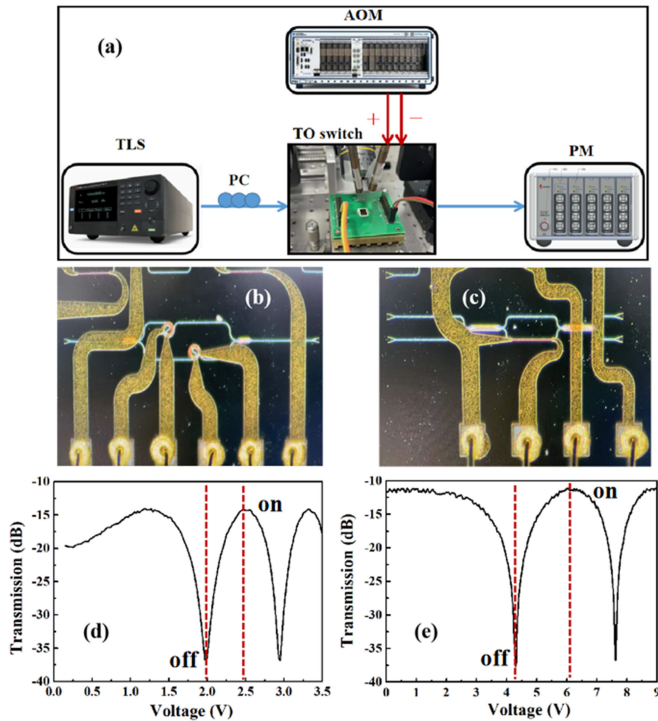


Fig. 5. (a) The experimental setup of switching power test. TLS: tunable laser source, PC: polarization controller, PM: power meter, AOM: analog output module. (b) The optical microscope image of the TO switch with spiral optical phase shifters. (c) The optical microscope image of TO switch with straight optical phase shifter. (d) The spiral waveguide TO switch's output with varying heating voltage. (e) The straight waveguide TO switch's output with varying heating voltage.

III. EXPERIMENTS AND DISCUSSION

We measured and compared the switching power of the TO switches with spiral and straight optical phase shifters in the same chip. The experimental set up is shown in Fig. 5(a), where the laser from a tunable laser source (TLS, Santac WSL-710) with output power of 0 dBm was injected into the TO switches with spiral and straight optical phase shifters separately, a power

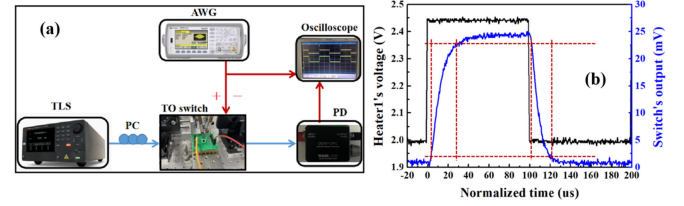


Fig. 6. (a) The experimental setup of switching time test. TLS: tunable laser source, PC: polarization controller, PD: photodetector, AWG: arbitrary waveform generator. (b) The measured switching time response with a 5 KHz square wave driving signal.

meter (PM, Santac MPM-210) was used to measure the optical power after the TO switches. By scanning the voltages applied on heater1 of the TO switches with an analog output module (AOM, NI PXIe-4322), the optical powers after the TO switches were measured. The optical microscope images of the TO switches with spiral and straight optical phase shifters are shown in Fig. 5(b) and (c). The measured transmissions versus the applied voltages on the TO switches with spiral and straight optical phase shifters are shown in Fig. 5(d) and (e), respectively. The results show that the “ V_{off} ” and “ V_{on} ” of the TO switch with spiral optical phase shifters are about 2.0 V and 2.46 V, respectively. The heater1's resistance is measured to be 235 Ω , the switching power of the TO switch with spiral phase shifters is about 8.73 mW, which can be obtained by (4):

$$P_{\text{switching}} = \frac{V_{\text{on}}^2 - V_{\text{off}}^2}{R_{\text{heater}}} \quad (4)$$

By contrast, the “ V_{off} ” and “ V_{on} ” of the MZI TO switch with straight optical phase shifter are about 4.3 V and 6.1 V, respectively. And the measured heater1's resistance is about 870 Ω , which corresponding to the switching power of about 21.5 mW. As can be seen, the switching power is reduced 59.4% by the spiral optical phase shifter, which matches the simulation results well. The insertion loss of the TO switch with spiral optical phase shifters is about 2 dB larger than that of the TO switch with straight optical phase shifter. According to our test, the insertion loss of both 1×2 MMI and 2×2 MMI are less than 0.5 dB, the additional insertion loss of TO switch with spiral optical phase shifters mainly comes from the spiral phase shifter. The transmission loss of the spiral phase shifter is about 1.2 dB, which is larger than the straight phase shifter. In the future optimization, the transmission loss of the spiral phase shifter can be further reduced by expanding the inner radius.

We also measured and compared the switching time responses of the TO switch with spiral optical phase shifters, without and with the optimized pulse driving. The experimental set up is shown in Fig. 6(a), where the laser from a TLS (Santac WSL-710) with output power of 10 dBm was injected into the TO switch, whose heaters' voltages are controlled by the arbitrary waveform generator (AWG, Keysight 33500B). And the AWG's output was also sent to the oscilloscope for reference. After the TO switch, a PD (Thorlabs DET01CFC) was adopted to convert optical signal into electronic signal, which is sent to the oscilloscope to obtain the TO switch's switching time

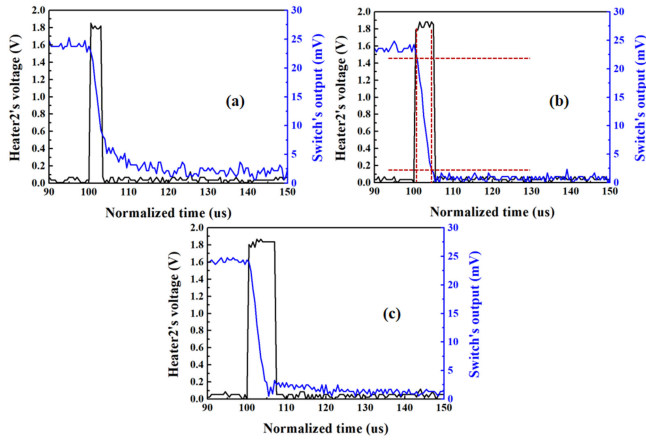


Fig. 7. (a) The measured “on” to “off” responses by applying a pulse on the heater2 with different pulse width. (a) $3\ \mu\text{s}$, (b) $5\ \mu\text{s}$, (c) $7\ \mu\text{s}$.

response. By applying a 5 KHz square wave signal with high level voltage of $V_{on} = 2.46\ \text{V}$ and low level voltage of $V_{off} = 2.0\ \text{V}$ to the heater1 of the TO switch, the TO switch’s switching time response without pulse driving was obtained as show in Fig. 6(b). The rise time (heating, 10%~90%) and fall time (cooling, 90%~10%) of the switch are $27\ \mu\text{s}$ and $22\ \mu\text{s}$, respectively.

Then we measured the switching time responses of the TO switch with the pulse driving. According to the theoretical modeling, an appropriate pulse voltage was applied on the heater2 to accelerate the cooling process and reduce the “on” to “off” switching time firstly. The measured heater2’s resistance is about $387\ \Omega$, according to (3), the pulse voltage applied on heater2 is about $1.84\ \text{V}$. We applied the pulse of $1.84\ \text{V}$ on the heater2 with pulse widths of $3\ \mu\text{s}$, $5\ \mu\text{s}$ and $7\ \mu\text{s}$, as the black curves shown in Fig. 7(a), (b) and (c). The corresponding switch’s “on” to “off” responses are shown as the blue curves in Fig. 7(a), (b) and (c). As can be seen, when the pulse width is set as $3\ \mu\text{s}$, the switch’s output is not reduced to minimum when the pulse ends, which means the pulse width is not enough. When the pulse width is set as $5\ \mu\text{s}$, the switch’s output is reduced to minimum and kept minimum when the pulse ends, which means the pulse width is suitable. This is consistent with our previous theory. When the pulse width is set as $7\ \mu\text{s}$, the switch’s output is reduced to minimum before the pulse ends, then additional ripple occurs, which means the pulse width is overloaded. Then, an optimized pulse voltage of $1.84\ \text{V}$ and $5\ \mu\text{s}$ pulse width is applied on the heater2 to accelerate the “on” to “off” process. The switch’s “on” to “off” switching time is reduced from $22\ \mu\text{s}$ to $4\ \mu\text{s}$, which is only about 18% of the switch’s response without the pulse driving. During the “on” to “off” process, the pulse voltage is only applied to the other arm in $5\ \mu\text{s}$, which is small compared to the on-off switching time of $22\ \mu\text{s}$ without pulse driving. No additional voltage needs to be applied to the other arm during other time. So this method is compatible with the case of simultaneous driving of both arms.

Base on the optimized “on” to “off” switching time of $4\ \mu\text{s}$, we then applied a pulse voltage on the heater1 to accelerated the

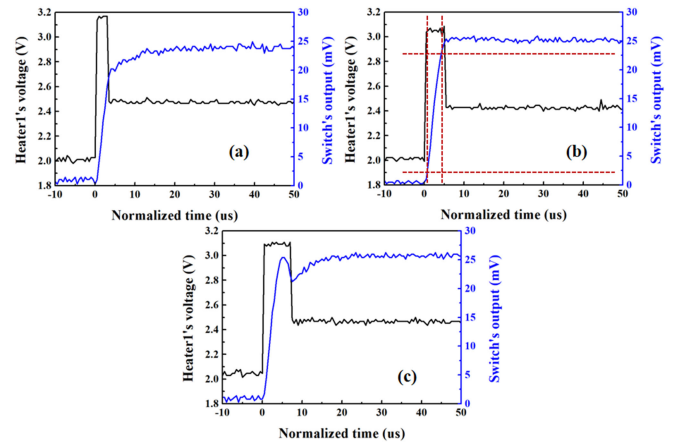


Fig. 8. (a) The measured “off” to “on” responses by applying a pulse on the heater1 with different pulse widths. (a) $3\ \mu\text{s}$, (b) $5\ \mu\text{s}$, (c) $7\ \mu\text{s}$.

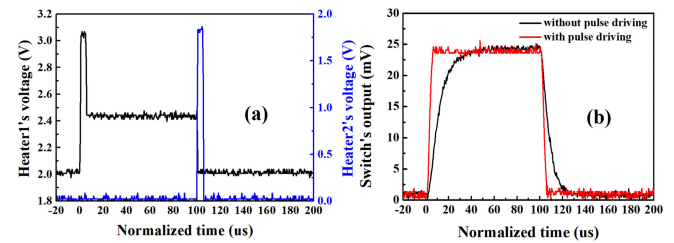


Fig. 9. (a) The optimized pulses applied on the two heaters of the TO switch with spiral optical phase shifter. (b) The TO switch’s switching time responses with and without the pulse driving.

“off” to “on” switching time into $4\ \mu\text{s}$. Here a pulse voltage with $3.1\ \text{V}$ amplitude was chosen to achieve “off” to “on” response, as shown in Fig. 8. When the pulse width is set as $3\ \mu\text{s}$, the switch’s output is not raised to maximum when the pulse ends, which means the pulse width is not enough. When the pulse width is set as $5\ \mu\text{s}$, the switch’s output is raised to maximum when the pulse ends, which means the pulse width is suitable. When the pulse width is set as $7\ \mu\text{s}$, the switch’s output is raised to maximum before the pulse ends and additional ripple occurs, which means the pulse width is overloaded. Then, an optimized pulse voltage of $3.1\ \text{V}$ and $5\ \mu\text{s}$ pulse width was applied on the heater1 to accelerate the “off” to “on” process. The measured switch’s “off” to “on” switching time is reduced from $27\ \mu\text{s}$ to $4\ \mu\text{s}$, which is only about 15% of the switch’s response without the pulse driving.

The experiments results show that both the switch’s “on” to “off” and “off” to “on” switching time can be reduced into $4\ \mu\text{s}$ by the optimized pulse driving. In other words, the switching time of the TO switch can be reduced from $27\ \mu\text{s}$ to $4\ \mu\text{s}$. Finally, we applied the optimized two pulse voltages as shown in Fig. 9(a) on both heaters of the TO switch simultaneously. The measured switching time response of the TO switch is shown as the red curve in Fig. 9(b). Comparing with the black curve in Fig. 9(b), which is the switching time response without the pulse driving, the switching time are dramatically reduced by the optimized pulse driving.

In the application scenarios where the TO switch keeps “on” or “off” state for a long time, the extra power consumption caused by the pulse voltage is low enough to be neglected because the pulse width of 5 μs is very small. In this case, the widely used $P_{\text{switching}}$ concept in (4) is still applicable. In the application scenarios where the TO switch’s “on” and “off” states need to be switched frequently, the additional power consumption should increase as the frequency of the main drive signal increases. If the frequency of the main drive signal is low, the additional power consumption will be a low level and the widely used $P_{\text{switching}}$ concept is still acceptable. If the frequency of the main drive signal increases, the widely used $P_{\text{switching}}$ concept may introduce some deviations. To compensate for these deviations, here we defined the extra power consumption in relation to the main drive signal frequency as follows. In the “off” to “on” process, the extra power consumption can be expressed as:

$$P_{\text{extra off-on}} = \frac{V_{\text{ph}}^2 - V_{\text{on}}^2}{R_1} \cdot a \quad (5)$$

Here a represents the ratio of pulse width with the “on” state, and can be expressed as:

$$a = \Delta t_{\text{pulse off-on}} / t_{\text{on}} = \Delta t_{\text{pulse off-on}} \cdot 2f \quad (6)$$

According to our experiment, $\Delta t_{\text{pulse on-off}} = 5 \mu\text{s}$, f represents the main drive signal frequency, it is also the switching frequency. If we set $f = 5 \text{ kHz}$ for example just as Fig. 9(a) shows, the extra power consumption for the “off” to “on” process is about 0.76 mW according to (5). If the main drive signal frequency is less than 5 kHz, the extra power consumption for the “off” to “on” process is less than 0.76 mW. Similarly, in the “on” to “off” process, the extra power consumption can be expressed as:

$$P_{\text{extra on-off}} = \frac{V_p^2}{R_2} \cdot b \quad (7)$$

Here b represents the ratio of pulse width applied on the other arm with the “off” state, and can be expressed as:

$$b = \Delta t_{\text{pulse on-off}} / t_{\text{off}} = \Delta t_{\text{pulse on-off}} \cdot 2f \quad (8)$$

According to our experiment, $\Delta t_{\text{pulse off-on}} = 5 \mu\text{s}$, we also set $f = 5 \text{ kHz}$ for example, the extra power consumption for the “on” to “off” process is about 0.44 mW according to (7). If the main drive signal frequency is less than 5 kHz, the extra power consumption for the “off” to “on” process is less than 0.44 mW. According to the above analysis, the overall extra power consumption relation to a 5 kHz main drive signal frequency is only 1.2 mW, and it is very small compared to 8.73 mW.

We compare the switching power and switching time of our work with the typical reported silicon TO switches without additional undercut process, as shown in Table I. Our TO switch with spiral optical phase shifters and optimized pulse driving can achieve sub-10 mW switching power and sub-10 μs switching time simultaneously. In future, our spiral waveguide structure can be further optimized to reduce the switching power, such as minimizing the gap among adjacent waveguides with different

TABLE I
THE PERFORMANCE COMPARISON BETWEEN OUR WORK AND OTHER
REPORTED SILICON TO SWITCHES

Ref	switching power (mW)	switching time (μs)
[14]	3.8 (with air-gap)	45
[15]	2.56	34.8
[16]	3	11
[18]	/	5.8
[19]	12.7	2.4
[20]	50	3.5
[21]	80	20
This work	8.73	4

waveguide widths in the spiral region, reducing the bend radius of the waveguide by adopting Euler curve or Clothoid bend [15], by these method, the size of the phase shifter can be more compact, longer waveguides can be heated directly by the heaters, which can further reduce the switching power. Furthermore, the pulse-width modulation in [18] could be adopted to avoid the requirement of digital to analog (DA) conversion and make the driving circuits simpler for the scenarios where large scale integration of TO switches are needed.

IV. CONCLUSION

In this paper, we designed and fabricated a silicon TO switch with spiral optical phase shifters, by adopting the spiral phase shifters instead of straight phase shifters, the switching power can be reduced from 21.5 mW to 8.73 mW. We also optimized the pulse driving, we proposed the calculation formula of the pulse voltage in the cooling process, and then the overall quantitative scheme of the pulse voltages and pulse widths in both cooling and heating processes. By adopting the optimized pulse driving, the switching time is reduced from 27 μs to 4 μs . In future, we will optimize spiral optical phase shifter more precisely to further reduce the switching power.

REFERENCES

- [1] W. N. Ye and Y. Xiong, “Review of silicon photonics: History and recent advances,” *J. Mod. Optic.*, vol. 60, no. 16, pp. 1299–1320, Jan. 2013.
- [2] Y. Su, Y. Zhang, C. Qiu, X. Guo, and L. Sun, “Silicon photonic platform for passive waveguide devices: Materials, fabrication, and applications,” *Adv. Mater. Technol.-US*, vol. 2, Jun. 2020, Art. no. 1901153.
- [3] W. Bogaerts and L. Chrostowski, “Silicon photonics circuit design: Methods, tools and challenges,” *Laser Photon. Rev.*, vol. 12, no. 4, Apr. 2018, Art. no. 1700237.
- [4] A. Rickman, “The commercialization of silicon photonics,” *Nat. Photon.*, vol. 8, no. 8, pp. 579–582, Aug. 2014.
- [5] X. Wang *et al.*, “Continuously tunable ultra-thin silicon waveguide optical delay line,” *Optica*, vol. 4, no. 5, pp. 507–515, Jan. 2017.
- [6] D. Lin *et al.*, “A tunable optical delay line based on cascaded silicon nitride microrings for Ka-band beamforming,” *IEEE Photon. J.*, vol. 11, no. 5, May 2019, Art. no. 5503210.
- [7] P. Zheng *et al.*, “A seven-bit silicon optical true time delay line for Ka-band phased array antenna,” *IEEE Photon. J.*, vol. 11, no. 4, Aug. 2019, Art. no. 5501809.
- [8] K. Tanizawa *et al.*, “Ultra-compact 32×32 strictly-non-blocking Si-wire optical switch with fan-out LGA interposer,” *Opt. Exp.*, vol. 23, no. 13, pp. 17599–17606, Jun. 2015.
- [9] J. Wang *et al.*, “Multidimensional quantum entanglement with large-scale integrated optics,” *Science*, vol. 360, no. 6386, pp. 285–291, Apr. 2018.

- [10] A. Liu *et al.*, "A high-speed silicon optical modulator based on a metal-oxide-semiconductor capacitor," *Nature*, vol. 427, pp. 615–618, Feb. 2004.
- [11] T. Hiraki *et al.*, "Heterogeneously integrated III–V/Si MOS capacitor Mach–Zehnder modulator," *Nat. Photon.*, vol. 11, pp. 482–485, Jul. 2017.
- [12] P. Sun and R. M. Reano, "Submilliwatt thermo-optic switches using freestanding silicon-on-insulator strip waveguides," *Opt. Exp.*, vol. 18, no. 8, pp. 8406–8411, Apr. 2010.
- [13] Y. Hashizume, S. Katayose, T. Tsuchizawa, T. Watanabe, and M. Itoh, "Low-power silicon thermo-optic switch with folded waveguide arms and suspended ridge structures," *Electron. Lett.*, vol. 48, no. 19, pp. 1234–1235, Sep. 2012.
- [14] K. Murray, Z. Lu, H. Jayatileka, and L. Chrostowski, "Dense dissimilar waveguide routing for highly efficient thermo-optic switches on silicon," *Opt. Exp.*, vol. 23, no. 15, pp. 19575–19585, Jul. 2015.
- [15] S. Chung, M. Nakai, and H. Hashemi, "Low-power thermo-optic silicon modulator for large-scale photonic integrated systems," *Opt. Exp.*, vol. 27, no. 9, pp. 13430–13459, Apr. 2019.
- [16] H. Qiu *et al.*, "Energy-efficient thermo-optic silicon phase shifter with well-balanced overall performance," *Opt. Lett.*, vol. 45, no. 17, pp. 4806–4809, Sep. 2020.
- [17] M. Harjanne, M. Kapulainen, T. Aalto, and P. Heimala, "Sub-us switching time in Silicon-on-Insulator Mach–Zehnder thermo-optic switch," *IEEE Photon. Technol. Lett.*, vol. 16, no. 9, pp. 2039–2041, Sep. 2004.
- [18] H. Matsuura *et al.*, "Accelerating switching speed of thermo-optic MZI silicon-photonic switches with 'Turbo pulse' in PWM control," in *Proc. Opt. Fiber Commun. Conf. Exhib. (OFC)*, Mar. 2017, pp. 1–3.
- [19] M. R. Watts, J. Sun, C. DeRose, D. C. Trotter, R. W. Young, and G. N. Nielson, "Adiabatic thermo-optic Mach–Zehnder switch," *Opt. Lett.*, vol. 38, no. 5, pp. 733–735, Mar. 2013.
- [20] R. L. Espinola, M.-C. Tsai, J. T. Yardley, and R. M. Osgood, "Fast and low-power thermo-optic switch on thin Silicon-on-Insulator," *IEEE Photon. Technol. Lett.*, vol. 15, no. 10, pp. 1366–1368, Oct. 2003.
- [21] L. Gu, W. Jiang, X. Chen, and R. T. Chen, "Thermooptically tuned photonic crystal waveguide Silicon-on-Insulator Mach–Zehnder interferometers," *IEEE Photon. Technol. Lett.*, vol. 19, no. 5, pp. 342–344, Mar. 2007.